CrossMark

ORIGINAL

**Marina Bošković · Radovan R. Bulatović · Slaviša Šalinić ·
Goran R. Miodragović · Gordana M. Bogdanović**

Optimization of dynamic quantities of a four-bar mechanism using the Hybrid Cuckoo Search and Firefly Algorithm (H-CS-FA)

Abstract This paper presents an optimization technique for dynamic balancing of a four-bar mechanism for the purpose of minimization of joint reactions, shaking forces and shaking moment. Joint reaction forces were determined by using a new method which can be applied in rigid planar closed-loop kinematic chains with revolute joints, and it is based on the use of absolute angles of rotation. The problem of balancing the obtained joint reaction forces was then solved as a multi-objective optimization problem. Kinematic and dynamic parameters of the four-bar linkage were taken as design variables. Three cases with simultaneous minimization of several objective functions were considered. The new hybrid algorithm named Hybrid Cuckoo Search and Firefly Algorithm (H-CS-FA) was used for solving the defined optimization problem in accordance with the given constraints. The appropriate selection of objective functions (three cases) and the application of the proposed algorithm resulted in a significant reduction of the values of joint reactions, shaking forces, shaking moment and driving torque. A concrete numerical example was used to show the efficiency of the new hybrid algorithm. The results obtained by H-CS-FA are compared with those obtained by using basic algorithms in the hybridization process (CS and FA) which proved the superiority of the newly proposed optimization procedure.

M. Bošković · R. R. Bulatović (✉) · S. Šalinić
Faculty of Mechanical and Civil Engineering in Kraljevo, University of Kragujevac, Dositejeva 19, 36000 Kraljevo, Serbia
E-mail: bulatovic.r@mfkv.kg.ac.rs; ukib@tron-inter.net

M. Bošković
E-mail: boskovic.m@mfkv.kg.ac.rs

S. Šalinić
E-mail: salinic.s@mfkv.kg.ac.rs

G. R. Miodragović
School of Mechanical Engineering of Applied Study Trstenik, Radoja Krstića 19, 37240 Trstenik, Serbia
E-mail: mijac037@yahoo.com

G. M. Bogdanović
Faculty of Engineering University of Kragujevac, University of Kragujevac, Sestre Janjić 6, 34000 Kragujevac, Serbia
E-mail: gocab@kg.ac.rs

1 Introduction

The problem of determination and optimization of joint reactions as well as minimization of shaking forces and shaking moment in different types of mechanisms represents a big challenge for researchers and designers. Mechanisms are required to operate uniformly even at high speeds. In order to accomplish it, it is necessary to reduce the forces and the moment which are the results of inertia. The minimization of shaking forces and shaking moment leads to improved dynamics, while noise and vibrations decrease. Besides, the determination of joint reactions plays an important role in stress analysis and dimensioning of mechanisms. Šalinić [1] proposed an algorithm for determination of joint reactions in a symbolic form in planar and spatial rigid multibody systems.

Mechanisms can be balanced either statically or dynamically. The condition for achieving static balance is that the sum of all forces during motion must equal zero [2]. In order to achieve the balance of forces, it is necessary to have the stationary mass center. Static balancing is accomplished by using the method of counterweights [3] or the method of mass redistribution [4]. Berkof and Lowen [5] proposed the method of linearly independent vectors, which requires redistribution of masses of members in such a way that the total center of mass becomes stationary. Arakelian and Dahan [6] introduced a method for complete balancing of the shaking force and partial balancing of the shaking moment which is applied for any planar or spatial mechanism. The method is based on the principle of minimization of the mean value of the shaking moment.

Dynamic balancing implies simultaneous balancing of shaking forces and the moment [7,8]. In order to satisfy dynamic balance, the sum of all forces and the sum of all moments must be equal to zero. The use of counterweights and counter-rotations for shaking force and shaking moment balancing leads to the increase in mass and inertia of the mechanism. Since recently, several optimization techniques have been used for minimization of shaking moment only, or, in combination with the minimization of shaking force, and/or driving torque. In addition to conventional optimization techniques which are applied for optimal balancing of planar mechanisms [9], modern evolutionary optimization techniques, which are biologically inspired, are often applied. Dynamic balancing of a planar mechanism in which shaking forces and shaking moment are minimized by using the Genetic Algorithm, GA, is considered in [10]. Minimization of shaking forces and the moment by finding the optimal distribution of mass of mechanism members by using an equivalent system of point-masses is described in [10,11]. Chaudhary et al. [11] solved the multi-objective optimization problem by using the teaching-learning-based optimization (TLBO) algorithm. Farmani et al. [12] considered the problem of dynamic balancing in a four-bar mechanism by using two evolutionary algorithms called non-dominated sorting Genetic Algorithm and multi-objective particle swarm optimization. The objective functions were derived from the concept of inertia counterweights and physical pendulum that permit complete balance of all mass effects.

For the purpose of obtaining as good results as possible and as effective algorithms as possible, and in addition to the modification of standard optimization algorithms, several authors also combined two and more different optimization algorithms.

A certain number of papers deal with the problem of balancing and optimization of dynamic parameters of a four-bar mechanism. Guo et al. [13] proposed a new method which represents a combination of the mass redistribution method and the counterweight method for a planar four-bar mechanism. For the purpose of reducing shaking forces, shaking moment and driving torque, the proposed method used the Genetic Algorithm. Erkaya [14] presented a practical method for reducing shaking forces and fluctuation of the moment in a four-bar mechanism, which is based on the Genetic Algorithm. It was shown that the structure of the objective function and the values of weighting factors have an important role in the optimization process.

The problem of minimization of joint reactions was discussed in [15,16]. Šalinic et al. [15] presented two ways for minimization of joint reactions of a planar serial manipulator. The first way is based on the optimal selection of the angular rotation laws of manipulator links, and the second one on attaching counterweights to the manipulator links. Harl, Oblak and Butinar [16] considered the minimization of joint reactions of planar kinematic chains by means of a multi-objective approach. The attention is directed toward the formulation of the problem of nonlinear programming for the purpose of minimization of generalized forces.

In several papers, there is a reference to the research done so far, with an overview of the literature in this field and the summary of results obtained by different methods of balancing of mechanisms. Arakelian and Smith [17] presented an overview of methods for dynamic balancing of mechanisms based on the generation of different movements of counterweights. Complete shaking force and shaking moment balancing are demonstrated using the pantograph copying properties. Wijk and Herder [18] presented the balancing principles which are obtained from a survey of the literature and applied them to a representative mechanism. They summarized and compared

the existing balancing principles concerning the addition of mass and the addition of inertia. Zhang and Wei [7] provided a detailed description of modern technologies and principles of dynamic balancing of mechanisms based on the minimum increase in mass and inertia. Also, they explained the synthesis of parallel robots on the basis of decomposition and the concept of integration. Several chapters of the book are devoted to the discussion and presentation of optimization processes which are applied in balancing of mechanisms.

This paper considers the problem of dynamic balancing of a four-bar mechanism which is presented in Fig. 1. The masses of the links are m_1, m_2 and m_3, while the lengths of the links are L_1, L_2 and L_3. The four-bar mechanism is placed in the vertical plane $O_1 x y$. The positions of the mass centers C_p ($p = 1, 2, 3$) are defined by α_p[rad]id_p[m], ($p = 1, 2, 3$).

Firstly, the joint reactions were determined at all joints by using the new method which can be applied to rigid planar closed-loop kinematic chains. The problem of dynamic balancing of mechanisms was then solved as an optimization problem. Unlike some papers [10,14,15] in which one objective function was formed by using weighting factors, the optimization problem in this paper is solved by using a multi-objective approach.

In this paper, two biologically inspired algorithms, Cuckoo Search—CSA (Yang in [19]) and Firefly Algorithm—FA (Yang and Deb in [20]), i.e., their hybridization, are used for solving the problem of multi-objective optimization. Almost all biologically inspired algorithms are of recent origin, and they look simple and their main characteristics are most often derived, directly or indirectly, on the basis of observations of systems from nature. The success and popularity of these algorithms can be attributed to the following factors: simplicity of algorithm, simplicity of application and diversity of solutions they generate.

Several biologically inspired algorithms are capable of achieving convergence toward a global optimum of an optimization problem after a relatively small number of iterations. This characteristic practically recommends them for solving problems of global optimization. To be efficient, biologically inspired algorithms must have certain specific characteristics. They must generate new solutions which are better than the previous ones. The second characteristic is that a metaheuristic algorithm must recognize a trap of entering a local optimum and have a mechanism which will take it out of that search space. A good combination of these characteristics results, under certain conditions, in a good efficiency of the algorithm, which, again, requires good balance of two main components: intensification and diversification [21]. Diversification means that different solutions which search the space on a global scale are generated, whereas intensification means to focus on the search in a local region using the information about good solutions found in it. Intensification often uses randomization, which enables the algorithm to leave any local minimum. It can also be used for local search around the currently best solution if the step is restricted to a local region. If the step is sufficiently big, randomization can explore the search space on a global scale.

The number of biologically inspired algorithms has been rapidly rising recently, so that the short research by Fister in [22] shows that there are more than 40 kinds of these algorithms with the tendency of appearance of new ones inspired by nature. It is simply impossible to mention all the existing types of biologically inspired algorithms, as well as their modifications and hybridizations. Readers can find a detailed overview of the existing algorithms in the paper written by Yang [23].

The application of biologically inspired algorithms in the design of mechanisms can be seen in the following papers: [24–33].

Except biologically inspired algorithms, gradient-based methods can effectively lead to a global optimum. However, gradient-based methods involve determination of the first and the second derivative of the objective
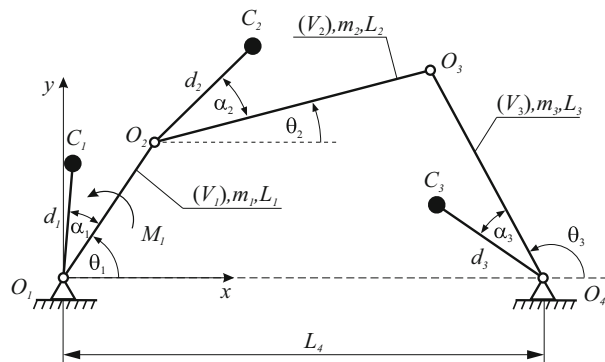

Fig. 1 A general four-bar mechanism

function and that is not always easy in real engineering problems. In addition, the use of gradient-based methods to a complex optimization problems is limited because it is necessary to set the initial values of the design variables in such a way to make them close to the desired (optimum) values. In some cases, the gradient must be approximated numerically which is not at all an easy task because it requires several additional calculations of the objective function in each iteration. Due to the above facts, the authors did not deal with the application of this algorithm, leaving the space for future research.

As aforementioned, this paper shows how a multi-objective optimization problem was solved by using a new algorithm created by hybridization of two biologically inspired algorithms—Cuckoo Search and Firefly Algorithm, i.e., H-CS-FA. The selected algorithms have different approaches and optimization flows, but what they have in common is that both of them use the mechanism of Lévy flights for obtaining solutions. [34,35]. The main difference between these two algorithms is that in the CS algorithm there is a mechanism for elimination of a "bad" nest, which represents a danger that the algorithm may, at a point, leave the good direction while searching for an optimum solution, which can lead to the increased time of finding the optimum.

In the H-CS-FA algorithm, a new approach for solving the problem of multi-objective optimization is introduced where simultaneous, i.e., parallel search is used. After starting the initial solution for each objective function, it is checked whether the optimality criterion is satisfied for every pass. If the optimality criterion is not satisfied for all objective functions, the algorithm starts checking from the beginning, in a new iteration. Otherwise, i.e., when the optimality criterion is satisfied for all objective functions, that solution is proclaimed the best one and the values of the objective function are compared with it in the next iterative cycle. The risk of wrong estimation of the values of weight factors for each objective function is thus avoided, i.e., the search time is reduced—the cycle of searching for the best values of each objective function is avoided because everything is done in one iterative cycle of searching.

The paper is organized as follows: Section 2 provides a detailed description of the new method for determination of joint reactions. Solving of the problem of dynamic balancing by applying multi-objective optimization and the new hybrid algorithm H-CS-FA is presented in Sect. 3. The efficiency of the new hybrid algorithm was tested on the example of optimization of dynamic parameters of a four-bar mechanism and the obtained results are shown in Sect. 4. Finally, the conclusions and notes are presented in Sect. 5.

2 A new method for determination of joint reactions of a four-bar mechanism

This section will present a new method for determination of joint reaction forces in rigid planar closed-loop kinematic chains in which rigid bodies are interconnected by revolute joints. This new method is based on the approach for determination of joint reaction forces in tree structure rigid multibody systems described in [1]. Namely, in our paper the method from [1] will be modified and extended to the case of rigid planar closed-loop multibody systems. The modification of the method from [1] relates to the use of absolute angles of rotation of bodies in the kinematic chain instead of relative angles of rotation between neighboring bodies connected by a revolute joint. In terms of calculation, the use of absolute angles of rotation considerably simplifies the procedure of determination of joint reaction forces in comparison with the procedure from [1] based on relative joints coordinates.

According to [36], after cutting off the joint O_3 (see Fig. 1), the motion of the considered four-bar mechanism can be divided into simultaneous motions of two mechanisms denoted with I and II and shown in Fig. 2, where the links of the mechanism II are massless.

The driving torques M_1^*, M_2^* and M_3^* act in the joints O_1, O_2 and O_4 of the mechanism I, while in the mechanism II the corresponding driving torques are M_1^{**}, M_2^{**} and M_3^{**}, respectively. Since the joints O_2, O_3 and O_4 of the four-bar mechanism shown in Fig. 1 are passive (not actuated), the following conditions must be satisfied [36]:

$$M_2^* + M_2^{**} = 0 \tag{1}$$
$$M_3^* + M_3^{**} = 0 \tag{2}$$

External force systems exerted on the links (V_p) $(p = 1, 2, 3)$ of the mechanism I are represented by equivalent force systems consisting of forces $\mathbf{F}_p^*$ $(p = 1, 2, 3)$ determined by:

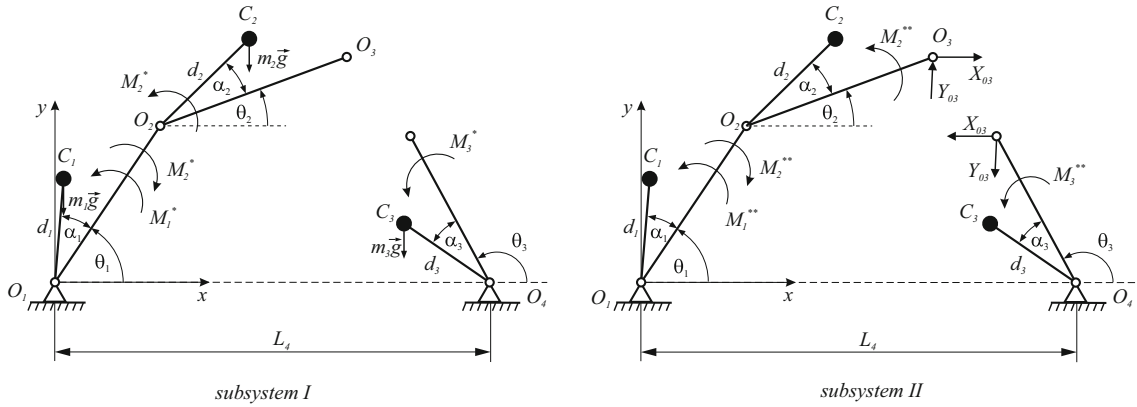$$\mathbf{F}_p^* = \begin{bmatrix} 0 & -m_p g & 0 \end{bmatrix}, p = 1, 2, 3 \tag{3}$$

Fig. 2 The four-bar mechanism equivalently represented through two subsystems I and II
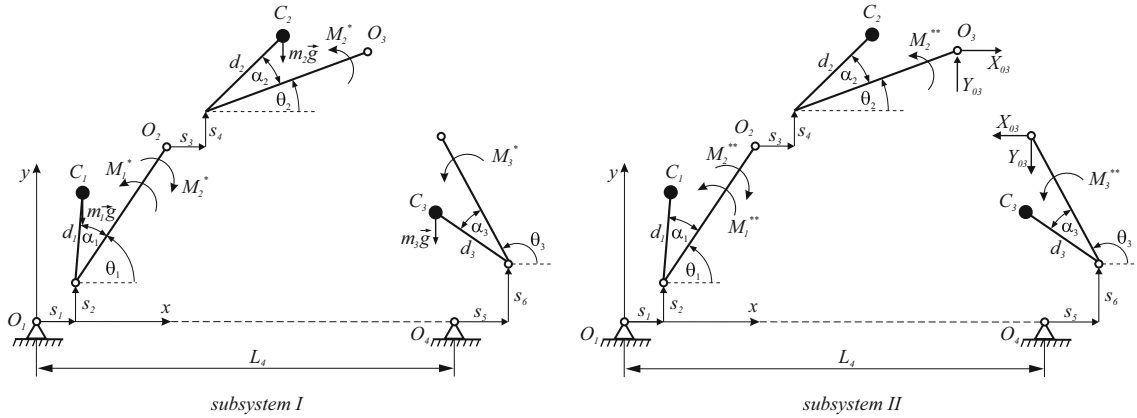

Fig. 3 The introduction of redundant coordinates in the mechanisms I and II

passing through the mass centers C_p ($p = 1, 2, 3$), respectively, together with the couples with torques $\mathbf{M}_p^*$ ($p = 1, 2, 3$) given by:

$$\mathbf{M}_1^* = \begin{bmatrix} 0 & 0 & M_1^* - M_2^* \end{bmatrix}, \tag{4}$$

$$\mathbf{M}_2^* = \begin{bmatrix} 0 & 0 & M_2^* \end{bmatrix}, \tag{5}$$

$$\mathbf{M}_3^* = \begin{bmatrix} 0 & 0 & M_3^* \end{bmatrix}, \tag{6}$$

where g is the gravitational acceleration.

Similarly, for the mechanism II one has:

$$\mathbf{F}_1^{**} = \begin{bmatrix} 0 & 0 & 0 \end{bmatrix}, \tag{7}$$

$$\mathbf{F}_2^{**} = \begin{bmatrix} X_{O_3} & Y_{O_3} & 0 \end{bmatrix}, \tag{8}$$

$$\mathbf{F}_3^{**} = \begin{bmatrix} -X_{O_3} & -Y_{O_3} & 0 \end{bmatrix}, \tag{9}$$

$$\mathbf{M}_1^{**} = \begin{bmatrix} 0 & 0 & M_1^{**} - M_2^{**} \end{bmatrix}, \tag{10}$$

$$\mathbf{M}_2^{**} = \begin{bmatrix} 0 & 0 & M_2^{**} + X_{O_3} (d_2 \sin (\theta_2 + \alpha_2) - L_2 \sin \theta_2) + Y_{O_3} (-d_2 \cos (\theta_2 + \alpha_2) + L_2 \cos \theta_2) \end{bmatrix}, \tag{11}$$

$$\mathbf{M}_3^{**} = \begin{bmatrix} 0 & 0 & M_3^{**} + X_{O_3} (-d_3 \sin (\theta_3 + \alpha_3) + L_3 \sin \theta_3) - Y_{O_3} (-d_3 \cos (\theta_3 + \alpha_3) + L_3 \cos \theta_3) \end{bmatrix}, \tag{12}$$

where X_{O_3} and Y_{O_3} represent the components of reaction force in the joint O_3 along the x and y axes, respectively. In accordance with [37,38], introducing now redundant coordinates $s_1, \ldots, s_6$ (also known as open-constraint coordinates), the motions of the mechanisms I and II can be described by the generalized coordinates $q_1, \ldots, q_9$ where $q_i \equiv \theta_i$ ($i = 1, 2, 3$) and $q_{3+r} \equiv s_r$ ($r = 1, \ldots, 6$) and where the following constraints hold (see Fig. 3):

$$f_r \equiv q_{3+r} = 0, \quad r = 1, \ldots, 6. \tag{13}$$

Note that the coordinates $s_1, \ldots, s_6$ represent the prohibited relative motions in the joints O_1, O_2 and O_4. In addition, the constraints (13) may be written at velocity and acceleration levels, respectively, as follows:

$$\dot{q}_{3+r} \equiv 0, \quad \ddot{q}_{3+r} \equiv 0, \quad r = 1, \ldots, 6. \tag{14}$$

Applying Kane's equations with undetermined multipliers [39] for the mechanism I, one has:

$$Q_{i(*)}^a + Q_{i(*)}^{in} = 0, \quad i = 1, 2, 3 \tag{15}$$

$$Q_{3+r(*)}^a + Q_{3+r(*)}^{in} + \lambda_{r(*)} = 0, \quad r = 1, \ldots, 6 \tag{16}$$

and for the mechanism II:

$$Q_{i(**)}^a + Q_{i(**)}^{in} = 0, \quad i = 1, 2, 3 \tag{17}$$

$$Q_{3+r(**)}^a + Q_{3+r(**)}^{in} + \lambda_{r(**)} = 0, \quad r = 1, \ldots, 6 \tag{18}$$

where $Q_{j(*)}^a$ $(j = 1, \ldots, 9)$ and $Q_{j(**)}^a$ $(j = 1, \ldots, 9)$ represent generalized active forces corresponding to the generalized coordinates $q_1, \ldots, q_9$ determined by the following expressions:

$$Q_{j(*)}^a = \sum_{p=1}^{3} \left(\mathbf{M}_p^* \frac{\partial \boldsymbol{\omega}_p}{\partial \dot{q}_j} + \mathbf{F}_p^* \frac{\partial \mathbf{V}_{C_p}}{\partial \dot{q}_j} \right), \quad j = 1, \ldots, 9 \tag{19}$$

$$Q_{j(**)}^a = \sum_{p=1}^{3} \left(\mathbf{M}_p^{**} \frac{\partial \boldsymbol{\omega}_p}{\partial \dot{q}_j} + \mathbf{F}_p^{**} \frac{\partial \mathbf{V}_{C_p}}{\partial \dot{q}_j} \right), \quad j = 1, \ldots, 9 \tag{20}$$

$Q_{j(*)}^{in}$ $(j = 1, \ldots, 9)$ and $Q_{j(**)}^{in}$ $(j = 1, \ldots, 9)$ are the generalized inertia forces corresponding to the generalized coordinates $q_1, \ldots, q_9$ determined by:

$$Q_{j(*)}^{in} = -\sum_{p=1}^{3} \left(m_p \mathbf{a}_{C_p}^T \frac{\partial \mathbf{V}_{C_p}}{\partial \dot{q}_j} + J_{C_p} \boldsymbol{\varepsilon}_p^T \frac{\partial \boldsymbol{\omega}_p}{\partial \dot{q}_j} \right), \quad j = 1, \ldots, 9 \tag{21}$$

$$Q_{j(**)}^{in} = 0, \quad j = 1, \ldots, 9 \tag{22}$$

In the expressions (19)–(21), $\boldsymbol{\omega}_p = \begin{bmatrix} 0 & 0 & \dot{\theta}_p \end{bmatrix}^T$ and $\boldsymbol{\varepsilon}_p = \begin{bmatrix} 0 & 0 & \ddot{\theta}_p \end{bmatrix}^T$ are the angular velocity and the angular acceleration of the link (V_p), respectively, $\mathbf{V}_{C_p} = \begin{bmatrix} \dot{x}_{C_p} & \dot{y}_{C_p} & 0 \end{bmatrix}^T$ and $\mathbf{a}_{C_p} = \begin{bmatrix} \ddot{x}_{C_p} & \ddot{y}_{C_p} & 0 \end{bmatrix}^T$ are the linear velocity and the linear acceleration of the mass center C_p, respectively, where the Cartesian coordinates x_{C_p} $(p = 1, 2, 3)$ and y_{C_p} $(p = 1, 2, 3)$ are given in Appendix, and J_{C_p} is the mass moment of inertia about centroidal axis of the link (V_p).

Solving now Eqs. (15) and (17) for M_2^*, M_2^{**}, M_3^* and M_3^{**} and substituting the obtained quantities into Eqs. (1) and (2) yield the following expressions for the components of the reaction force in the joint O_3:

$$\begin{aligned}
X_{O_3} = -\frac{1}{2L_2L_3\cos(\theta_2 - \theta_3)} & \Big[d_2 L_1 L_3 m_2 \left(\cos(\alpha_2 - \theta_1 + \theta_2 - \theta_3) + \cos(\alpha_2 - \theta_1 + \theta_2 + \theta_3) \right) \ddot{\theta}_1 \\
& + 2 \left(d_2^2 L_3 m_2 + J_{C_2} L_3 \right) \ddot{\theta}_2 \cos\theta_3 + 2L_2 \left(J_{C_3} + m_3 d_3^2 \right) \ddot{\theta}_3 \cos\theta_2 \\
& + d_2 L_1 L_3 m_2 \dot{\theta}_1^2 \left(\sin(\alpha_2 - \theta_1 + \theta_2 - \theta_3) \right. \\
& + \sin(\alpha_2 - \theta_1 + \theta_2 + \theta_3)) + d_2 g L_3 m_2 \left(\cos(\alpha_2 + \theta_2 - \theta_3) + \cos(\alpha_2 + \theta_2 + \theta_3) \right) \\
& + d_3 g L_2 m_3 \left(\cos(\alpha_3 - \theta_2 + \theta_3) + \cos(\alpha_3 + \theta_2 + \theta_3) \right) \Big]
\end{aligned} \tag{23}$$

$$\begin{aligned}
Y_{O_3} = -\frac{1}{2L_2L_3\cos(\theta_2 - \theta_3)} & \Big[d_2 L_1 L_3 m_2 \left(\sin(\alpha_2 - \theta_1 + \theta_2 + \theta_3) - \sin(\alpha_2 - \theta_1 + \theta_2 - \theta_3) \right) \ddot{\theta}_1 \\
& + 2 \left(d_2^2 L_3 m_2 + J_{C_2} L_3 \right) \ddot{\theta}_2 \sin\theta_3 + 2L_2 \left(J_{C_3} + m_3 d_3^2 \right) \ddot{\theta}_3 \sin\theta_2 \\
& + d_2 L_1 L_3 m_2 \dot{\theta}_1^2 \left(\cos(\alpha_2 - \theta_1 + \theta_2 - \theta_3) \right. \\
& - \cos(\alpha_2 - \theta_1 + \theta_2 + \theta_3)) + d_2 g L_3 m_2 \left(\sin(\alpha_2 + \theta_2 + \theta_3) - \sin(\alpha_2 + \theta_2 - \theta_3) \right) \\
& + d_3 g L_2 m_3 \left(\sin(\alpha_3 + \theta_2 + \theta_3) - \sin(\alpha_3 - \theta_2 + \theta_3) \right) \Big]
\end{aligned} \tag{24}$$

where the constraints (14) are taken into account. In addition, from Eq. (16) it follows that:

$$\lambda_{1(*)} = m_1 \left(\ddot{x}_{C_1}\right)_0 + m_2 \left(\ddot{x}_{C_2}\right)_0, \tag{25}$$

$$\lambda_{2(*)} = (m_1 + m_2) \, g + m_1 \left(\ddot{y}_{C_1}\right)_0 + m_2 \left(\ddot{y}_{C_2}\right)_0, \tag{26}$$

$$\lambda_{3(*)} = m_2 \left(\ddot{x}_{C_2}\right)_0, \tag{27}$$

$$\lambda_{4(*)} = m_2 g + m_2 \left(\ddot{y}_{C_2}\right)_0, \tag{28}$$

$$\lambda_{5(*)} = m_3 \left(\ddot{x}_{C_3}\right)_0, \tag{29}$$

$$\lambda_{6(*)} = m_3 g + m_3 \left(\ddot{y}_{C_3}\right)_0, \tag{30}$$

and from Eq. (18):

$$\lambda_{1(**)} = \lambda_{3(**)} = -X_{O_3}, \tag{31}$$

$$\lambda_{2(**)} = \lambda_{4(**)} = -Y_{O_3}, \tag{32}$$

$$\lambda_{5(**)} = X_{O_3}, \tag{33}$$

$$\lambda_{6(**)} = Y_{O_3} \tag{34}$$

where the notation $(\cdot)_0$ means that the quantity $(\cdot)$ is calculated for $q_4 = \cdots = q_9 = 0$.

Finally, the components of reaction forces in the joints $O_1, \; O_2$ and O_4 along the x and y axes, respectively, read:

$$X_{O_1} = \lambda_{1(*)} + \lambda_{1(**)} = m_1 \left(\ddot{x}_{C_1}\right)_0 + m_2 \left(\ddot{x}_{C_2}\right)_0 - X_{O_3} \tag{35}$$

$$Y_{O_1} = \lambda_{2(*)} + \lambda_{2(**)} = m_1 \left(\ddot{y}_{C_1}\right)_0 + m_2 \left(\ddot{y}_{C_2}\right)_0 + (m_1 + m_2) \, g - Y_{O_3} \tag{36}$$

$$X_{O_2} = \lambda_{3(*)} + \lambda_{3(**)} = m_2 \left(\ddot{x}_{C_2}\right)_0 - X_{O_3} \tag{37}$$

$$Y_{O_2} = \lambda_{4(*)} + \lambda_{4(**)} = m_2 \left(\ddot{y}_{C_2}\right)_0 + m_2 g - Y_{O_3} \tag{38}$$

$$X_{O_4} = \lambda_{5(*)} + \lambda_{5(**)} = m_3 \left(\ddot{x}_{C_3}\right)_0 + X_{O_3} \tag{39}$$

$$Y_{O_4} = \lambda_{6(*)} + \lambda_{6(**)} = m_3 \left(\ddot{y}_{C_3}\right)_0 + m_3 g + Y_{O_3} \tag{40}$$

In Eqs. (23), (24) and (35)–(40), the quantities θ_2 and θ_3 and their time derivatives can be eliminated using the following relations [2]:

$$\theta_2 = 2 \tan^{-1} \left(\frac{-b_2 \pm \sqrt{b_2^2 - 4a_2 c_2}}{2a_2} \right) \tag{41}$$

$$\theta_3 = 2 \tan^{-1} \left(\frac{-b_3 \pm \sqrt{b_3^2 - 4a_3 c_3}}{2a_3} \right) \tag{42}$$

where

$$a_2 = \cos\theta_1 - \frac{L_4}{L_1} + \frac{L_4}{L_2} \cos\theta_1 + \frac{L_3^2 - L_4^2 - L_1^2 - L_2^2}{2L_1 L_2}, \tag{43}$$

$$b_2 = -2 \sin\theta_1, \tag{44}$$

$$c_2 = \frac{L_4}{L_1} + \left(\frac{L_4}{L_2} - 1 \right) \cos\theta_1 + \frac{L_3^2 - L_4^2 - L_1^2 - L_2^2}{2L_1 L_2}, \tag{45}$$

$$a_3 = \cos\theta_1 - \frac{L_4}{L_1} - \frac{L_4}{L_3} \cos\theta_1 + \frac{L_1^2 - L_2^2 + L_3^2 + L_4^2}{2L_1 L_3}, \tag{46}$$

$$b_3 = -2 \sin\theta_1, \tag{47}$$

$$c_3 = \frac{L_4}{L_1} - \left(\frac{L_4}{L_3} + 1 \right) \cos\theta_1 + \frac{L_1^2 - L_2^2 + L_3^2 + L_4^2}{2L_1 L_3}, \tag{48}$$

At the end, it should be added that the presented approach for determination of joint reactions in planar closed-loop multibody systems is based on the technique of introducing prohibited relative motions in the joints, as in the approach described in [40]. However, our approach in terms of calculation is advantageous over the approach in [40] because it does not require the formation of constraint Jacobian matrices and their pseudo-inverse matrices, as in [40]. In this paper, this is allowed by using one absolute coordinate (absolute angle of rotation), and not three as in [40], for determination of the position of links of the mechanism.

3 Optimization process

3.1 Hybrid Cuckoo Search and Firefly Algorithm (H-CS-FA)

The algorithm used in this paper was created by hybridization of two biologically inspired algorithms: Cuckoo Search and Firefly Algorithm.

Cuckoo Search (CS) represents a new optimization metaheuristic algorithm, which is also biologically inspired by the cuckoos' manner of looking for nests where they could lay eggs. This algorithm, as already said, was proposed by Yang and Deb in [19]. The Cuckoo Search algorithm is a biologically inspired algorithm which is widely applied in solving very complex optimization problems in various fields of engineering, industry, etc. In the existing literature, there are a large number of papers where this algorithm was used in its original form, or as its various improvements or hybridizations with other algorithms. A detailed presentation of application of the standard Cuckoo Search algorithm can be seen in the review articles [41–43].

The Firefly Algorithm (FA) was introduced for the first time by Yang, in [20]. The Firefly Algorithm is also a biologically inspired optimization algorithm which idealizes some characteristics of the flashing light of the firefly. A comprehensive review of the literature where the Firefly Algorithm was applied for solving different optimization problems was given by Fister et al. in [44] and Yang and Xingshi in [45].

In this paper, the authors will not remain on a detailed explanation of these algorithms.

The hybrid algorithm applied in this paper represents a combination of the Cuckoo Search algorithm, CS, and the Firefly Algorithm, FA. In both algorithms, generation of new solutions takes place according to the Lévy flight mechanism. The main difference between these two algorithms is that in the CS algorithm there is a mechanism of elimination of a "bad" nest, which represents a danger that the algorithm may, at a point, leave the good direction while searching for an optimum solution. It can lead to the increased time of finding the optimum.

The proposed hybrid algorithm is based on the CS algorithm which incorporates a part of the FA, which is shown in Algorithm 1.

Algorithm 1. Pseudo code of H-CS-FA algorithm

1:	Objective function $F(\mathbf{X})$, $\mathbf{X} = \left(x_1, x_2, ..., x_d\right)^T$
2:	Defining the number of parameters that optimize d
3:	Defining the number of iterations $iter$ max
4:	Defining the boundaries of design variables $\%\%$ upper UB and lower boundaries LB
5:	Defining the number of nests, n
6:	Initialization of the population of the n nest $x_{j,i}$ $\left(i=1,2,...,n\right)$, $\left(j=1,2,...,d\right)$,
7:	Initialization of first best solutions, F_{min}
8:	*while* $\left(t < iter \, \text{max}\right)$
9:	Calculation of the quality cuckoo choices by the Lévy flight, F_i
10:	$F_{new} = min\left(F\right)$
11:	Random selection among the n generated nests (j-th nest)
12:	$\%\%$ *inserted part of the FA*
13:	*if* $\left(F_i > F_j\right)$
14:	Replace j-th nest with the new solution
15:	*end if*

```
16:        for i=1:n   %% all n nests
17:            for j=1:n   %% all n nests
18:                if (F_j > F_i)
19:                    Moving i–th cuckoo in j –direction in d -dimensional space
20:                    Varying the attractiveness of the distance r via exp[-γr]
21:                    Calculation of new solutions and updating the brightness
22:                end if
23:            end for j
24:        end for i
25:        F_new = min(F)
26:        if(F_new < F_min)
27:            Accepting the new solution, F_min = F_new
28:        end if
29:    Ranking fireflies and finding the currently best solution
30:    end while
31:    Post-processing and presentation of results
```

MOO is used for solving optimization problems which include two or more complex, nonlinear, opposed objective functions, which should be simultaneously optimized: min $\{F_1(X), F_2(X), \ldots, F_m(X),\}$ where X is the vector of design variables: $\mathbf{X} = (x_1, x_2, \ldots, x_d)^T$. In single-criterion optimization, i.e., optimization with one objective function, the optimization algorithm generates a new solution looking for it in the search space defined by the boundaries of design variables. During the iterative process, worse solutions are eliminated and replaced with better ones. The solution found for that iterative cycle is also the best one for the given optimization problem. However, in nontrivial, MOO problems, there is no unique solution which will at the same time optimize each objective function. The optimum solutions found cannot be improved by one criterion without being worsened by another, which makes the search and finding of the optimum solution by all criteria considerably difficult.

In the literature, the method of weighting factors or the Pareto front is used for solving the problems of multi-objective optimization. In the method of weighting factors, all objective functions are transformed through weighting factor into one objective function and the problem of multi-objective optimization is reduced to the problem of single-criterion optimization. In the application of the Pareto front, instead of weighting factors, the best values for each objective function are used and those best values have the role of the weighting factor during the linearization of problems, i.e., transformation of multi-objective optimization into single-criterion optimization.

In this paper, simultaneous, i.e., parallel search is used for solving the problem of multi-objective optimization. After starting the initial solution for each objective function, it is checked whether the optimality criterion is satisfied for every pass. If the optimality criterion is not satisfied for all objective functions, the algorithm starts checking from the beginning, in a new iteration. Otherwise, i.e., when the optimality criterion is satisfied for all objective functions, that solution is proclaimed the best one and the values of the objective function are compared with it in the next iterative cycle (Algorithm 2). The risk of wrong estimation of the values of weight factors for each objective function is thus avoided, i.e., the search time is reduced—the cycle of searching for the best values for each objective function is avoided because everything is done in one iterative cycle of searching.

The shaded rows in Algorithm 2 show that from the matrix of solutions $n \times d$ where n—the number of nests and d—the number of design variables, only the solution in which all elements of the newly generated row of the matrix of solutions are smaller than the corresponding elements of the previous best solution is selected.

Algorithm 2. Pseudo code of H-CS-FA aghorithm at MOO

1:	Defining the number set of objective function, m
2:	Objective function $min\{F_1(\boldsymbol{X}), F_2(\boldsymbol{X}),..., F_m(\boldsymbol{X}),\}$, $\boldsymbol{X}=(x_1, x_2,..., x_d)^T$
3:	Defining the number of parameters that optimize d
4:	Defining the number of iterations $iter\,\mathrm{max}$
5:	Defining the boundaries of design variables %% upper UB and lower boundaries LB
7:	Defining the number of nests, n
8:	Initialization of the population of the n nest n nest $x_{j,i}$ $(i=1,2,...,n)$, $(j=1,2,...,d)$,
9:	Initialization of first best solutions for all objective functions, $F_{\min}=\{F_{\min 1}, F_{\min 2},..., F_{\min k}\}$
10:	**while** $(i<iter\,\mathrm{max})$
11:	**for** $k=1{:}m$ %% for all objective function
12:	Calculation of the quality cuckoo choices by the Lévy flight, $F_{i,k}$
13:	$F_{new}[k]=F_{newk}$,
14:	**next** k
15:	$F_{new}=min(F)$, $F_{new}=\{F_{new1}, F_{new2},..., F_{newk}\}$
16:	Random selection among the n generated nests (j-th nest)
17:	%% inserted part of the FA
18:	fulfil_the_condition=True
19:	**for** $k=1{:}m$ %% for all objective function
20:	**if** $(F_{newik}>F_{newjk})$,
21:	fulfil_the_condition=True
22:	**else**
23:	fulfil_the_condition=False
24:	**end if**
25:	**next** k
26:	**if** fulfil_the_condition
27:	Replace j-th nest with the new solution
28:	**end if**
29:	**for** $i=1{:}n$ %%all n nests
30:	fulfil_the_condition=True
31:	**for** $j=1{:}n$ %% all n nests
32:	**for** $k=1{:}m$ %% for all objective functions
33:	**if** $(F_{jk}>F_{ik})$,
34:	fulfil_the_condition=True
35:	**else**
36:	fulfil_the_condition=False
37:	**end if**
38:	**next** k
39:	**if** fulfil_the_condition
40:	Moving i–th cuskoo in j –direction in d -dimensional space
41:	Varying the attractiveness of the distance r via $exp[-\gamma r]$
42:	Calculation of new solutions and updating the brightness
43:	**end if**
44:	**end for** j
45:	**end for** i
46:	fulfil_the_condition=True
47:	**for** $k=1{:}m$ %% for all objective functions
48:	**if** $F_{new}[k]\le F_{min}[k]$,
49:	fulfil_the_condition=True
50:	**else**
51:	fulfil_the_condition=False
52:	**end if**
53:	**next** k
54:	**if** fulfil_the_condition
55:	Accepting the new solution, $(F_{min}=F_{new})$,
56:	**end if**
57:	Ranking fireflies and finding the currently best solution
58:	**end while**
59:	Post-processing and presentation of results

3.2 Objective function

There are two different approaches in multi-objective optimization. The first one uses specially structured algorithms whose goal is obtaining the best set of non-dominated solutions in terms of Pareto fronts. The second one is usually defined as multi-objective optimization, which consists of one optimization goal when different objective functions are linearly combined in a unique objective function using weighting factors. The authors of this paper follow the approach which differs from the above-mentioned two, where optimizations of several objective functions are performed simultaneously. Multi-objective optimization is applied for the minimization of joint reaction forces, shaking force, shaking moment and driving torque of a four-bar mechanism. Based on the above expressions, the problem is defined as follows:

$$\min \{F_1(X), F_2(X), \ldots, F_m(X)\} \tag{49}$$

Subject to: $g_j(X) \leq 0$, $j = 1, \ldots, k$ where $F_i(X)$, $(i = 1, 2, \ldots, m)$ is the objective functions, $g_j(X) \leq 0$, are the constraint functions and k is the number of constraints. The design variables vector is denoted by $X = (x_1, x_2, \ldots, x_d)^T$, and d is the number of design variables.

The upper and lower boundaries are defined for each design variable. Sixteen design variables are considered, and thus, X is defined as:

$$X = \left\{L_1, L_2, L_3, L_4, \alpha_1, \alpha_2, \alpha_3, m_1, m_2, m_3, J_{C_1}, J_{C_2}, J_{C_3}, d_1, d_2, d_3\right\} \tag{50}$$

and the boundaries of design variables are shown in Table 1.

4 Numerical results

In this paper, the problem of dynamic balancing of a four-bar mechanism is considered as a multi-objective optimization problem. The new algorithm, (H-CS-FA), is used for solving the optimization problem. The driving member 2 rotates with a constant angular velocity of 300 rpm.

The following three cases are considered:

Case 1—In this case, reactions are optimized at all four joints of the given mechanism, i.e., simultaneous minimization of eight objective functions is performed. Unlike numerous examples in the available literature in which only joint reactions in fixed joints, i.e., ground joint reaction forces, are optimized, the relations below show that the objective functions are selected in such a way to cover the reactions at all joints of the observed four-bar mechanism.

$$F_j = \frac{1}{\delta}\sqrt{\sum_{i=0}^{\delta} f_j^2(t_i)}, \quad j = (1, 2, \ldots, 8), \quad \text{where } \delta = 200, \quad \text{and } t = 0{:}0.01{:}0.2; \tag{51}$$

$$f_1 = X_{O1}, f_2 = Y_{O1}, f_3 = X_{O2}, f_4 = Y_{O2}, f_5 = X_{O3}, f_6 = Y_{O3}, f_7 = X_{O4}, f_8 = Y_{O4}, \tag{52}$$

Case 2—In this case, all joint reactions and the driving torque are optimized. In other words, nine objective functions are minimized simultaneously:

$$F_j = \frac{1}{\delta}\sqrt{\sum_{i=0}^{\delta} f_j^2(t_i)}, \quad j = (1, 2, \ldots, 9), \quad \text{where } \delta = 200, \quad \text{and } t = 0{:}0.01{:}0.2; \tag{53}$$

$$f_1 = X_{O1}, f_2 = Y_{O1}, f_3 = X_{O2}, f_4 = Y_{O2}, f_5 = X_{O3}, f_6 = Y_{O3}, f_7 = X_{O4}, f_8 = Y_{O4}, \; , f_9 = M_1 \tag{54}$$

Case 3—By applying the H-CS-FA algorithm in this case, three objective functions which cover the shaking forces in the direction of x and y axes, as well as the shaking moment, are simultaneously minimized:

$$F_j = \frac{1}{\delta}\sqrt{\sum_{i=0}^{\delta} f_j^2(t_i)}, \quad j = (1, 2, 3), \quad \text{where } \delta = 200, \quad \text{and } t = 0{:}0.01{:}0.2; \tag{55}$$

$$f_1 = F_{shx}, f_2 = F_{shy}, f_3 = M_{sh}, \tag{56}$$

Table 1 Original and optimized parameters of the four-bar mechanism

| Design variables	Original values (taken from [14])	Case 1			Case 2			Case 3			Boundaries
		FA	CS	H-CS-FA	FA	CS	H-CS-FA	FA	CS	H-CS-FA	
L_1 (m)	0.100	0.104	0.120	0.080	0.819	0.120	0.080	0.119	0.120	0.080	0.08–0.120
L_2 (m)	0.400	0.366	0.441	0.480	0.406	0.458	0.480	0.394	0.453	0.427	0.320–0.480
L_3 (m)	0.320	0.369	0.256	0.256	0.319	0.256	0.256	0.315	0.256	0.256	0.256–0.384
L_4 (m)	0.600	0.611	0.529	0.568	0.566	0.557	0.607	0.549	0.536	0.557	0.480–0.720
α_1 (rad)	0	0.422	3.642	3.197	1.974	2.998	2.982	3.063	3.023	3.144	0–$2 \times \pi$
α_2 (rad)	0	0.100	5.311	1.799	2.459	1.022	0.947	0.046	6.283	3.951	0–$2 \times \pi$
α_3 (rad)	0	0.862	5.711	2.482	1.465	4.476	1.583	5.992	1.990	1.984	0–$2 \times \pi$
m_1 (kg)	0.360	0.215	0.010	1.535	1.967	3.000	1.721	2.172	1.200	1.000	0.01–3
m_2 (kg)	1.296	1.326	1.000	0.800	0.923	0.800	0.831	1.434	1.600	1.010	0.8–1.6
m_3 (kg)	1.046	0.886	1.007	0.819	0.841	1.394	0.857	0.879	0.634	0.532	0.5–1.5
J_{C_1} (kgm²)	4.13×10^{-4}	34.39×10^{-4}	43.31×10^{-4}	30.634×10^{-4}	51.43×10^{-4}	49.04×10^{-4}	26.705×10^{-4}	55.59×10^{-4}	53.01×10^{-4}	45.156×10^{-4}	2×10^{-4}–60×10^{-4}
J_{C_2} (kgm²)	1.87×10^{-2}	4.07×10^{-2}	2×10^{-2}	5.575×10^{-2}	6.567×10^{-2}	3.39×10^{-2}	2.122×10^{-2}	2.5×10^{-2}	4.1×10^{-2}	2.191×10^{-2}	2×10^{-2}–7×10^{-2}
J_{C_3} (kgm²)	9.85×10^{-3}	13.47×10^{-3}	15.61×10^{-3}	8.001×10^{-3}	17.925×10^{-3}	9.98×10^{-3}	8.002×10^{-3}	14.23×10^{-3}	12.25×10^{-3}	10.101×10^{-3}	8×10^{-3}–18×10^{-3}
d_1(m)	0.050	0.016	0.072	0.048	0.034	0.057	0.0535	0.081	0.100	0.082	0.001–0.1
d_2(m)	0.200	0.070	0.086	0.041	0.025	0.807	0.048	0.049	0.116	0.007	0.001– 0.400
d_3(m)	0.160	0.044	0.0933	0.002	0.016	0.039	0.010	0.112	0.091	0.001	0.001–0.320
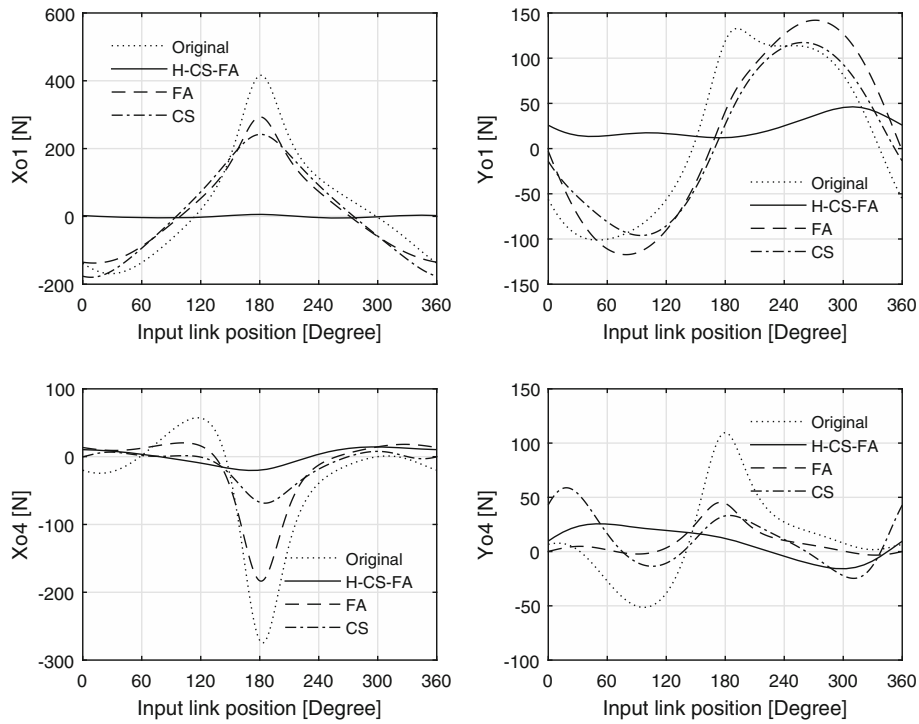
Fig. 4 Original and optimized values of ground joint reaction forces (Case 1)

The control parameters of the algorithm used in the optimization process for all three cases are:

$n = 25$—the number of nests; $p_a = 0.25$—the discovery rate of alien eggs; iter max $= 500$—the maximum number of iterations, $n_f = 40$—the number of fireflies, $\alpha = 0.5$—the randomization parameter, $\gamma = 1$—the absorption coefficient, $\beta_0 = 0.2$—the attractiveness, $d = 16$—the number of design variables.

Design variables are defined for the proposed mechanism. The non-optimized (original) values (taken from [14]) and the optimized values of design variables (obtained by using FA, CS and H-CS-FA), as well as the boundaries of design variables, are given in Table 1.

For Case 1, the ground joint reaction forces of the original and optimized mechanisms are given in Fig. 4. After the optimization process, the values of these forces are considerably lower in comparison with the initial values. The use of the above-mentioned optimization algorithm resulted in the reduction by 97.834%, 71.329%, 80.633% and 53.898%, in the values X_{O_1}, Y_{O_1}, X_{O_4} and Y_{O_4}, respectively.

Figure 5 presents the initial and optimized values of joint reactions at the movable joints O_2 and O_3. The reactions at these joints, X_{O_2}, Y_{O_2}, X_{O_3} and Y_{O_3} are reduced by 61.586%, 23.615%, 84.641% and 1.919%, respectively. On the other hand, Fig. 6 presents the change of values of the shaking forces, the shaking moment as well as the driving torque, before and after the optimization process, for Case 1.

In Case 2, the values of ground joint reaction forces which are considerably lower in comparison with the initial values are obtained by applying the H-CS-FA algorithm in the optimization process. In other words, the application of the hybrid algorithm results in the reduction by 90.293%, 69.216%, 84.639% and 72.665%, in the values X_{O_1}, Y_{O_1}, X_{O_4} and Y_{O_4}, respectively. Figure 7 presents the initial and optimized values of ground joint reaction forces for Case 2.

Similarly, the reactions at the movable joints X_{O_2}, Y_{O_2}, X_{O_3} and Y_{O_3} are reduced by 62.992%, 36.711%, 89.406% and 61.962%, respectively, while the optimized value of the driving torque is reduced by 92.546% in relation to the original value. The joint reactions at the movable joints O_2 and O_3 for Case 2 are presented in Fig. 8. The change of values of shaking forces along the axes x and y, the shaking moment as well as the driving torque, before and after the optimization process, for Case 2, is shown in Fig. 9.

The values of joint reactions, shaking forces, shaking moment and driving torque are considerably reduced by applying the proposed H-CS-FA algorithm in Case 3. The values of ground joint reaction forces X_{O_1}, Y_{O_1}, X_{O_4} and Y_{O_4} are reduced by 90.92%, 75.654%, 76.029% and 77.687%, respectively, in relation to the initial values. Figure 10 presents the original and optimized values of these reactions for Case 3 in the observed four-bar mechanism.
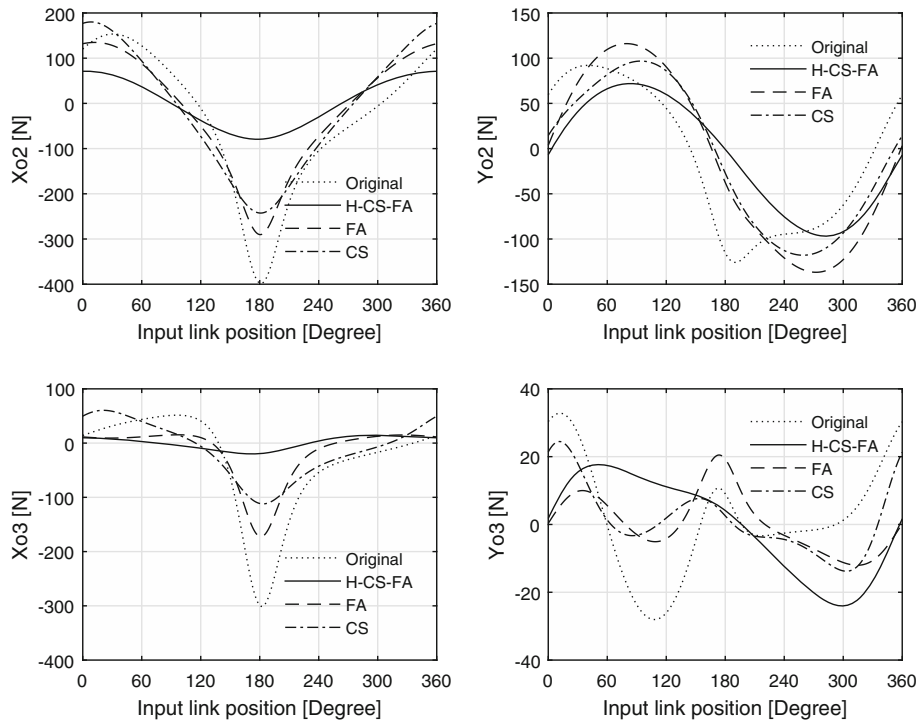
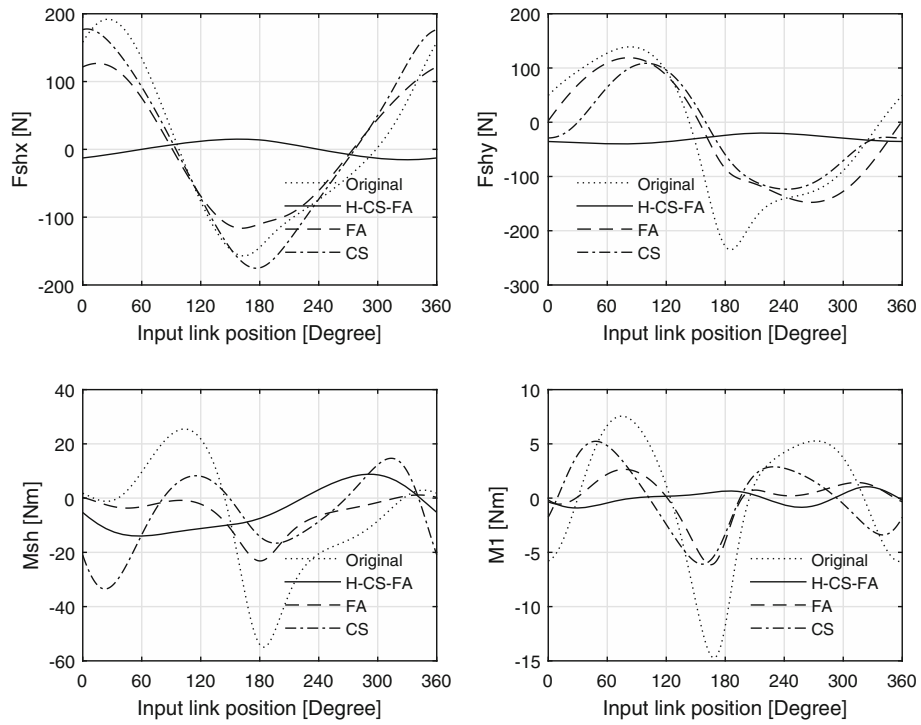**Fig. 5** Original and optimized values of reaction forces in the joints O_2 and O_3 (Case 1)

Fig. 6 Original and optimized values of shaking force components, shaking moment and driving torque (Case 1)
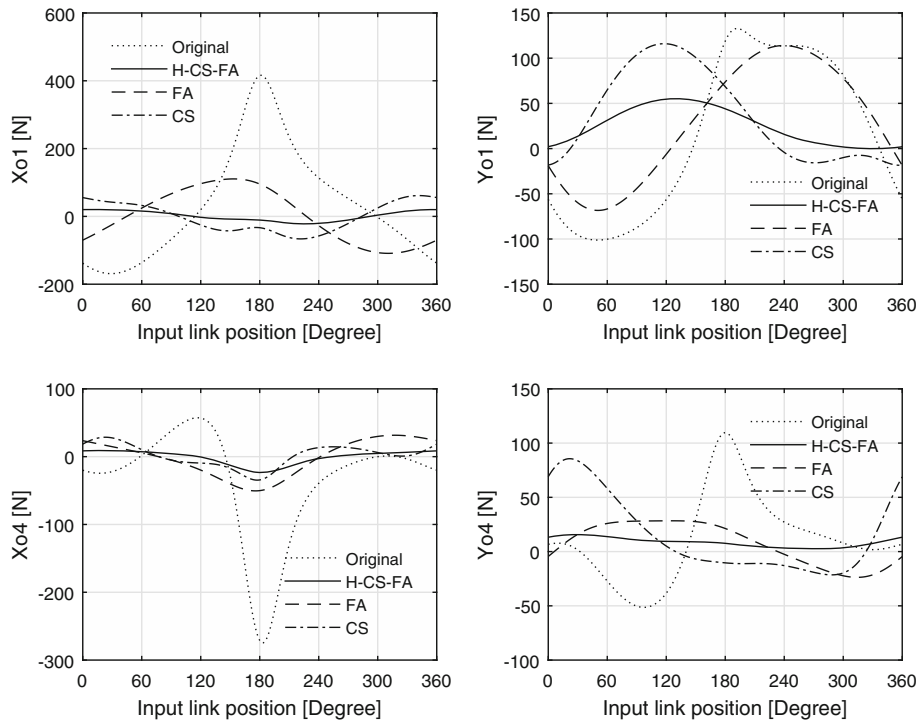
Fig. 7 Original and optimized values of ground joint reaction forces (Case 2)
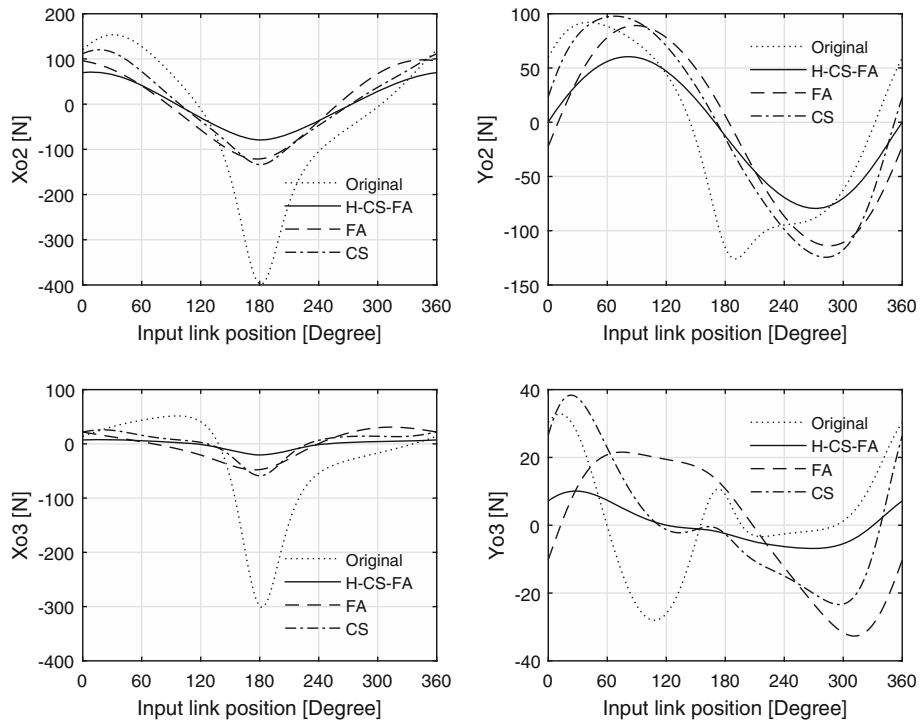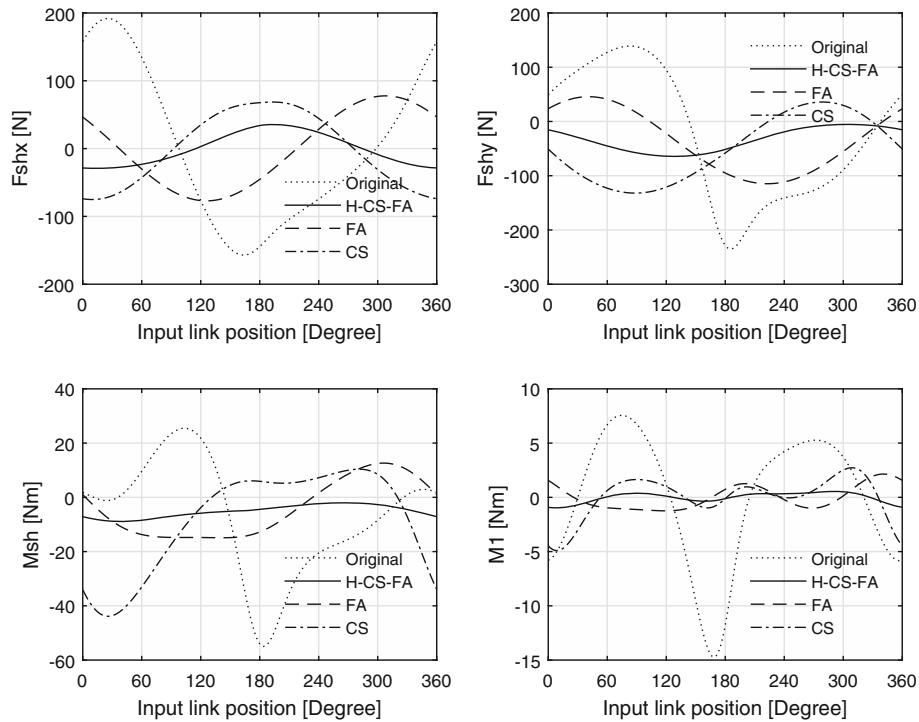

Fig. 8 Original and optimized values of reaction forces in the joints O_2 and O_3 (Case 2)

Fig. 9 Original and optimized values of shaking force components, shaking moment and driving torque (Case 2)

The joint reactions at the movable joints O_2 and O_3 in the original and optimized mechanisms are shown in Fig. 11. The application of the optimization process in Case 3 resulted in a considerable reduction of the values of these reactions, which is shown in Fig. 11. Also, after the optimization process and the application of the proposed algorithm, the values of shaking forces in the direction of x and y axes are reduced by 99.186% and 77.396%, while the value of the shaking moment M_{sh} is reduced by 76.383% in relation to the initial value. Figure 12 presents the original and optimized values of shaking forces, shaking moment and driving torque for Case 3.

Based on the optimal values of design variables given in Table 1, Figs. 4, 5, 6, 7, 8, 9, 10, 11 and 12 are obtained.

Observing Table 1, it can be noticed that several optimized values of design variables $(L_1, L_2, L_3, m_2, J_{C_3}, d_3)$ coincide with the lower or upper bounds of these variables. For this reason, the search space has been expanded, i.e., the boundaries of these design variables are expanded in order to test the sensitivity of the proposed algorithm.

The optimized values of design variables along with the expanded boundaries of these design variables are shown in Table 2. It should be noted that the expansion of the search space was done only for Case 3 in order to test the applied algorithm in terms of the speed of convergence and the sensitivity of the boundaries.

The italics values in Table 2 indicate the boundaries for the initial values of design variables with expanded range. As it can be seen from Table 2 by expanding the search space, i.e., by setting wider limits, the optimized values of design variables do not coincide with the lower or upper bounds of these variables.

The diagrams of convergence in this paper are given in Figs. 13, 14 and 15, only for Case 3. The diagrams of convergence in Figs. 13a, 14a and 15a correspond to the situation where the search space is within the boundaries of Table 1, while the diagrams of convergence in Figs. 13b, 14b and 15b correspond to the case where the search space is expanded (the boundaries of the design variables taken from Table 2). The other diagrams of convergence are not shown in order not to exceed the usual size of the paper.
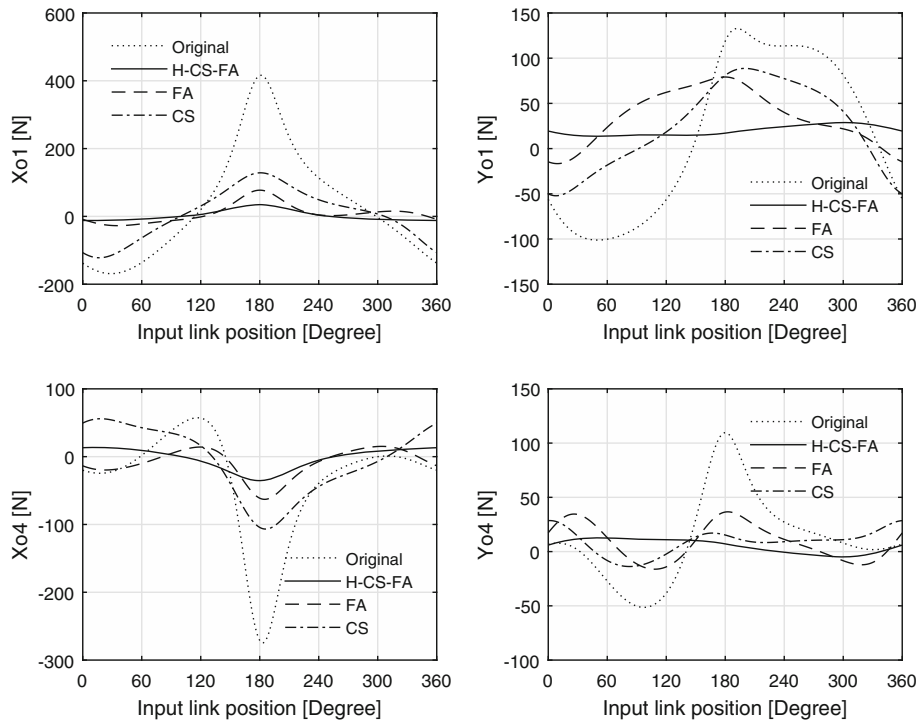
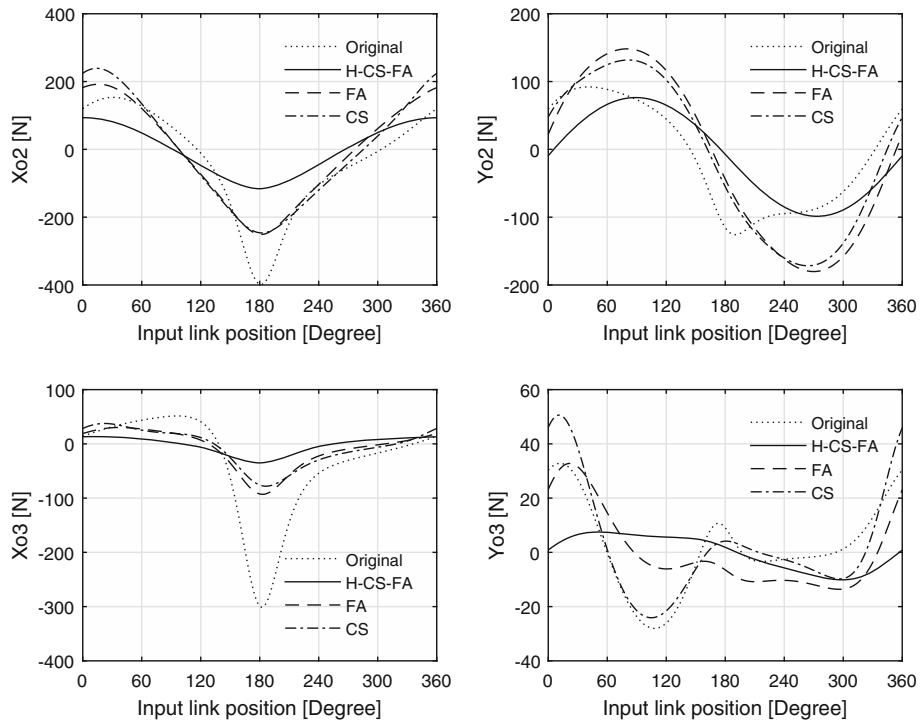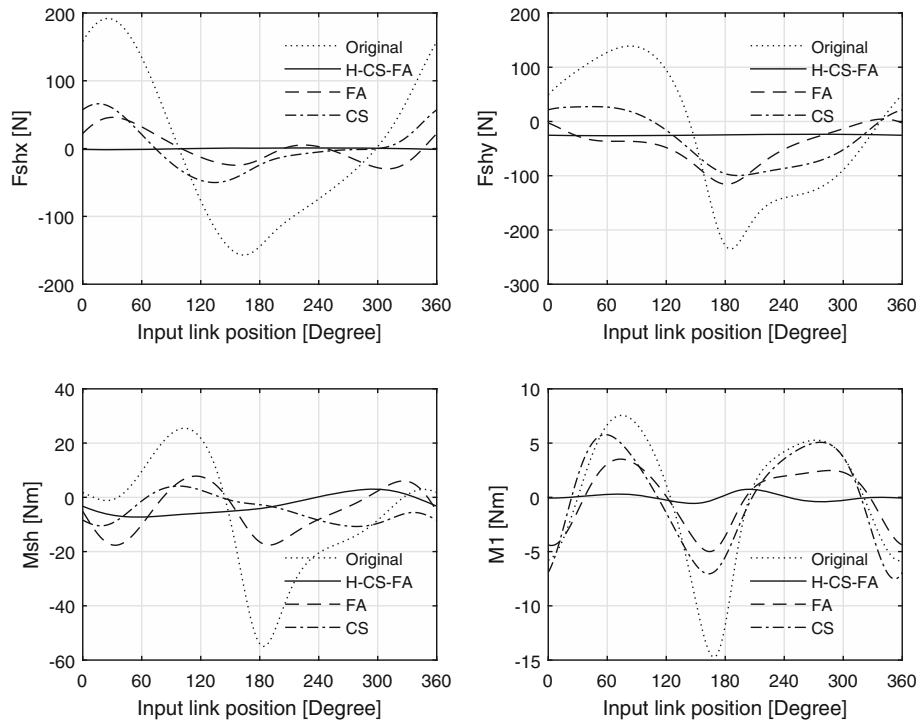**Fig. 10** Original and optimized values of ground joint reaction forces (Case 3)

Fig. 11 Original and optimized values of reaction forces in the joints O_2 and O_3 (Case 3)

Fig. 12 The original and optimized values of the shaking force components, the shaking moment and the driving torque (Case 3)

Table 2 Original and optimized parameters of the four-bar mechanism for expanded search space

Case 3			
Design variables	Original values (taken from [14])	H-CS-FA	Boundaries
L_1 (m)	0.100	0.064	*0.04–0.120*
L_2 (m)	0.400	0.518	*0.320–0.680*
L_3 (m)	0.320	0.174	*0.100–0.384*
L_4 (m)	0.600	0.584	0.480–0.720
α_1 (rad)	0	3.223	$0-2 \times \pi$
α_2 (rad)	0	5.543	$0-2 \times \pi$
α_3 (rad)	0	2.876	$0-2 \times \pi$
m_1 (kg)	0.360	1.040	0.01–3
m_2 (kg)	1.296	0.847	*0.6–1.6*
m_3 (kg)	1.046	0.560	0.5–1.5
J_{C_1} (kgm^2)	4.13×10^{-4}	23.214×10^{-4}	$2 \times 10^{-4} - 60 \times 10^{-4}$
J_{C_2} (kgm^2)	1.87×10^{-2}	3.56×10^{-2}	$2 \times 10^{-2} - 7 \times 10^{-2}$
J_{C_3} (kgm^2)	9.85×10^{-3}	16.32×10^{-3}	*$6 \times 10^{-3} - 18 \times 10^{-3}$*
d_1 (m)	0.050	0.0527	0.001–0.1
d_2 (m)	0.200	0.0804	0.001–0.400
d_3 (m)	0.160	0.00057	*0.0005–0.320*

It can be seen from the previous figures that the expansion of the search space does not significantly affect the speed of convergence. In gradient-based methods, by narrowing the search space, or by setting the initial values of the design variables in such a way to make them close to optimal, the speed of convergence is rapidly increasing. However, it should be noted that in H-CS-FA applied in this paper, the expansion of the search space does not significantly affect the speed of convergence. On the contrary, for one of the objective function (M_{sh}) the speed of convergence is better in the case of expanded boundaries (Fig. 15).

The percentage decreases of the values of joint reactions, the driving torque, the shaking force, and the shaking moment for all three considered cases are presented in Table 3. Note that two variants have been considered for Case 3: the search space with the boundaries from Table 1 and the expanded search space with
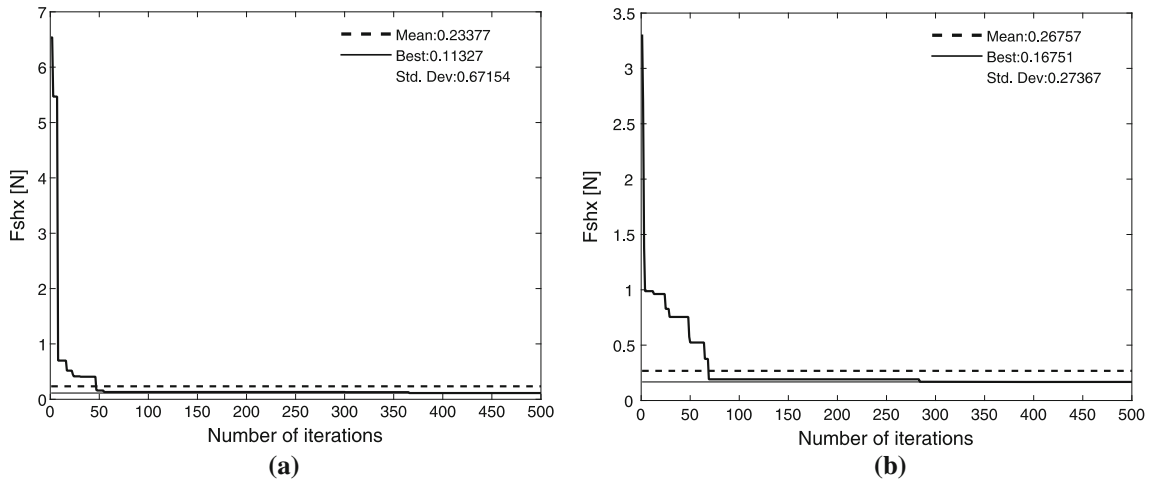
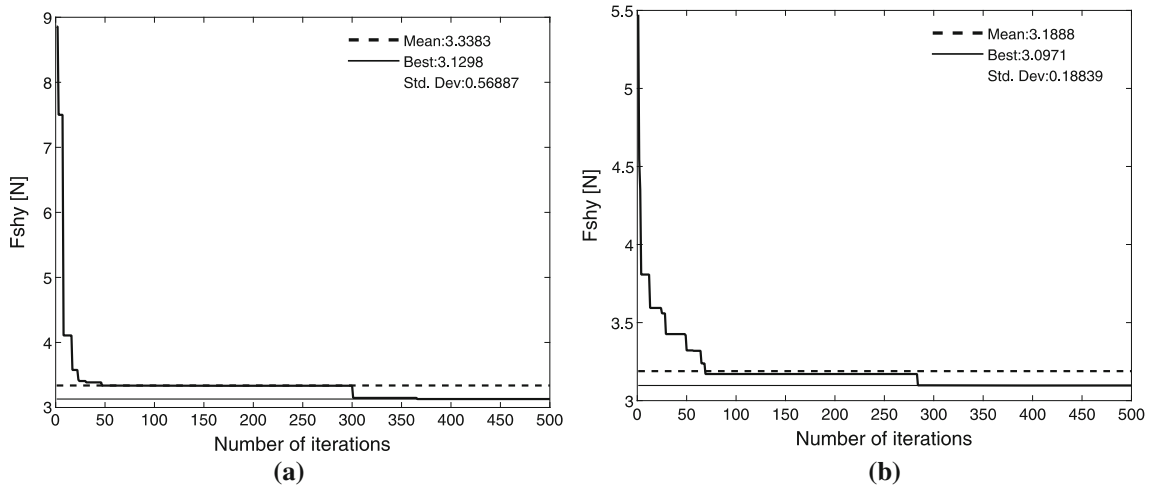**Fig. 13** Diagram of convergence in Case 3 for F_{shx}

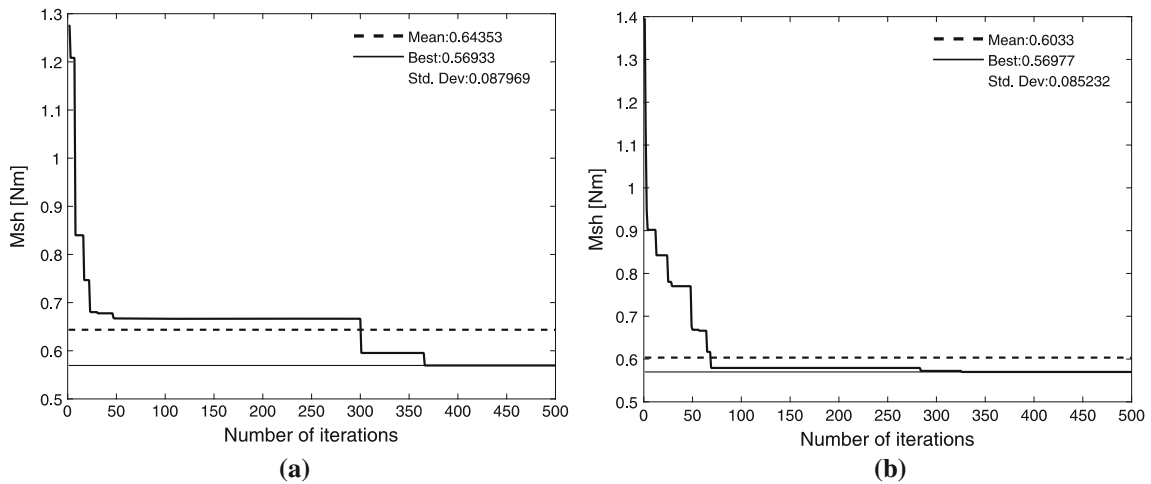**Fig. 14** Diagram of convergence in Case 3 for F_{shy}

Fig. 15 Diagram of convergence in case 3 for M_{sh}

Table 3 The decreasing ratios for the cases considered

Percentage decrease in values in relation to the original ones (%)

	Case 1			Case 2			Case 3			
	FA	CS	**H-CS-FA**	FA	CS	**H-CS-FA**	FA	CS	**H-CS-FA (Table 1)**	**H-CS-FA (Table 2)**
$X_{O_1}[N]$	18.862	11.868	**97.834**	47.768	71.270	**90.293**	84.250	52.94	90.920	78.148
$Y_{O_1}[N]$	6.583	13.554	**71.329**	24.376	43.401	**69.216**	52.392	44.504	75.654	78.449
$X_{O_2}[N]$	13.803	4.415	**61.586**	45.107	43.507	**62.992**	2.602	10.843	48.323	49.284
$Y_{O_2}[N]$	18.329	0.904	**23.615**	6.952	1.943	**36.711**	53.680	42.945	20.381	53.846
$X_{O_3}[N]$	51.530	34.565	**84.641**	66.442	71.774	**89.406**	58.284	57.238	80.744	56.743
$Y_{O_3}[N]$	*41.902*	*38.198*	**1.919**	40.919	18.896	**61.962**	6.287	15.653	54.004	69.616
$X_{O_4}[N]$	34.515	70.755	**80.633**	56.957	74.490	**84.639**	67.804	18.934	76.029	46.395
$Y_{O_4}[N]$	*66.865*	33.413	**53.898**	40.632	9.603	**72.665**	49.635	59.394	77.687	78.915
$M_1[Nm]$	70.061	44.981	90.317	81.166	71.922	**92.546**	52.759	21.615	94.762	81.788
$F_{\mathrm{sh}x}[N]$	21.432	4.292	90.385	50.261	52.053	79.055	81.238	73.805	**99.186**	**98.853**
$F_{\mathrm{sh}y}[N]$	17.343	36.838	71.947	48.487	41.272	69.698	59.69	56.217	**77.396**	**78.234**
$M_{\mathrm{sh}}[Nm]$	*65.140*	30.427	51.629	39.912	10.770	69.338	52.416	65.564	**76.383**	**77.178**

Bold values indicates the objective functions which are optimized in Case 1, 2 or 3

the bounds from Table 2. By expanding the boundaries of design variables for Case 3, the percentage decrease in values of objective functions ($F_{\mathrm{sh}x}$, $F_{\mathrm{sh}y}$ and M_{sh}) remains almost at the same level.

Note that the italics values presented in Table 3 represent the results obtained by individual application of the FA and CS algorithms, which are better in comparison with the corresponding results obtained by applying the H-CS-FA algorithm. Finally, by analyzing the data in Table 3, it can be concluded that for all three considered cases (Case 1, Case 2, and Case 3), the application of H-CS-FA results in the reduction of all optimization values. Also, for Case 1 and Case 2, in comparison with FA and CS, the H-CS-FA algorithm provides, for most optimization values, a higher degree of reduction in values of these quantities. In Case 2, in comparison with CS and FA, the use of the H-CS-FA algorithm results in a considerable reduction of all optimization values. From the aspect of minimization of reaction forces in the inner joints (joints 2 and 3) for the considered type of planar mechanism, it is best, for practical calculations, to use the objective function (49) composed of the particular functions defined in Case 2

5 Conclusions

This paper considers the problem of minimization of joint reactions, shaking forces, shaking moment and driving torque in a four-bar mechanism. Firstly, the joint reactions are determined by using a new method based on the use of absolute angles of rotation of the links. The problem of minimization of joint reactions is solved by using multi-objective optimization. Unlike the conventional approaches to multi-objective optimization which imply the use of weighting factors or the Pareto front, this paper presents a new algorithm created by means of hybridization of two biologically inspired algorithms in order to accomplish simultaneous minimization of several objective functions. Three cases in which eight, nine and three objective functions are simultaneouly minimized by optimization of the distribution of mass of each link of the mechanism are considered. The new biologically inspired algorithm, named Hybrid Cuckoo Search and Firefly Algorithm (H-CS-FA), is applied for the purpose of minimization of joint reaction forces, shaking force, shaking moment and driving torque. The results obtained show considerable reduction of values of these dynamic quantities in comparison with the original (non-optimized) ones. By analyzing the results shown in Table 3, it can be noticed that the greatest reduction in the value of the shaking force along the x and y axes, the shaking moment as well as the driving torque is in Case 3. Hence, in Case 3, when $F_{\mathrm{sh}x}$, $F_{\mathrm{sh}y}$ and M_{sh} are chosen for objective functions, the results show that their percentage decrease is also the highest. By expanding the search space, this result does not change significantly. In other words, by expanding the boundaries of design variables in Case 3, a percentage reduction in values $F_{\mathrm{sh}x}$, $F_{\mathrm{sh}y}$ and M_{sh} remains at the same level. In Case 1, where joint reactions at all joints are selected as objective functions in the optimization process, it can be noticed that there is the greatest reduction in the values of joint reactions in the stationary support O_1. In Case 2, where all joint reactions and the driving torque are optimized, it is noticed that the highest percentage decrease in joint reactions is in the joints O_2, O_3 and O_4. The imposed conclusion is that an adequate selection of objective functions can influence the degree of

reduction in the corresponding dynamic quantities. Also, the results obtained show that the use of the proposed H-CS-FA in the process of multi-objective optimization results in obtaining considerably reduced values of the optimized quantities, which proves its efficiency. Also, by comparing the results obtained using the hybrid algorithm (H-CS-FA) and the results obtained by applying the basic algorithms (CS and FA), the efficiency of the proposed optimization procedure and justification of the application of the proposed algorithm have been proved. While solving the problem of dynamic balancing of the four-bar mechanism in this paper, the joint reactions at all four joints are taken into account, which is not the case in the previous approaches in the literature which have considered only reaction forces at the ground joints, O_1 and O_4. Further research of the authors of this paper will be directed toward the extension of the proposed hybrid algorithm to other types of planar mechanisms.

Appendix

The Cartesian coordinates of mass centers C_p $(p = 1, 2, 3)$ of the mechanisms $\left(V_p\right)$ $(p = 1, 2, 3)$ of the mechanism shown in Fig. 3 are:

$$
\begin{aligned}
x_{C_1} &= s_1 + d_1 \cos\left(\theta_1 + \alpha_1\right), \\
y_{C_1} &= s_2 + d_1 \sin\left(\theta_1 + \alpha_1\right), \\
x_{C_2} &= s_1 + L_1 \cos\theta_1 + s_3 + d_2 \cos\left(\theta_2 + \alpha_2\right), \\
y_{C_2} &= s_2 + L_1 \sin\theta_1 + s_4 + d_2 \sin\left(\theta_2 + \alpha_2\right), \\
x_{C_3} &= L_4 + s_5 + d_3 \cos\left(\theta_3 + \alpha_3\right), \\
y_{C_3} &= s_6 + d_3 \sin\left(\theta_3 + \alpha_3\right).
\end{aligned}
$$

References

1. Šalinić, S.: Determination of joint reaction forces in a symbolic form in rigid multibody systems. Mech. Mach. Theory **46**, 1796–1810 (2011)
2. Norton, R.: Design of Machinery—An Introduction to the Synthesis and Analysis of Mechanisms and Machines. McGraw-Hill, New York (2004)
3. Walker, M.J., Oldhamn, K.: A general theory of force balancing using counterweights. Mech. Mach. Theory **13**, 175–185 (1978)
4. Tepper, F.R., Lowen, G.G.: General theorems concerning full force balancing of planar mechanisms by internal mass redistribution. ASME J. Eng. Ind. **94**(3), 789–796 (1972)
5. Berkof, R.S., Lowen, G.G.: A new method for completely force balancing simple linkages. ASME J. Eng. Ind. **91**, 21–26 (1969)
6. Arakelian, V., Dahan, M.: Partial shaking moment balancing of fully force balanced linkages. Mech. Mach. Theory **36**, 1241–1252 (2001)
7. Zhang, D., Wei, B.: Dynamic Balancing of Mechanisms and Synthesizing of Parallel Robots. Springer, Switzerland (2016)
8. Chaudhary, H., Saha, S.K.: Dynamic and Balancing of Multibody Systems. Springer, Berlin (2009)
9. Chaudhary, H., Saha, S.K.: Balancing of four-bar linkages using maximum recursive dynamic algorithm. Mech. Mach. Theory **42**, 216–232 (2007)
10. Chaudhary, K., Chaudhary, H.: Dynamic balancing of planar mechanisms using genetic algorithm. J. Mech. Sci. Technol. **28**, 4213–4220 (2014)
11. Chaudhary, K., Chaudhary, H.: Optimal dynamic design of planar mechanisms using teaching-learning-based optimization algorithm. J. Mech. Sci. Technol. **29**, 5189–5198 (2015)
12. Farmani, M.R., Jaamialahmadi, A., Babaie, M.: Multiobjective optimization for force and moment balance of a four-bar linkage using evolutionary algorithms. J. Mech. Sci. Technol. **25**, 2971–2977 (2011)
13. Guo, G., Morita, N., Torii, T.: Optimum dynamic design of planar linkage using genetic algorithm. JSME Int. J. C-Mech. Syst. **43**, 372–377 (2000)
14. Erkaya, S.: Investigation of balancing problem for a planar mechanism using genetic algorithm. J. Mech. Sci. Technol. **27**, 2153–2160 (2013)
15. Šalinić, S., Bošković, M., Bulatović, R.R.: Minimization of dynamic joint reaction forces of the 2-dof serial manipulators based on interpolating polynomials and counterweights. Theor. Appl. Mech. **42**, 249–260 (2015)
16. Harl, B., Oblak, M., Butinar, B.: Minimization of joint reaction forces of kinematic chains by a multi-objective approach. Struct. Multidiscip. Optim. **27**, 243–249 (2004)

17. Arakelian, V.H., Smith, M.R.: Shaking force and shaking moment balancing of mechanisms: a historical review with new examples. ASME J. Mech. Des. **127**, 334–339 (2005)
18. Wijk, V.V., Herder, J.L., Demeulenaere, B.: Comparison of various dynamic balancing principles regarding additional mass and additional inertia. ASME J. Mech. Robot. **1**(4), 041006 (2009). https://doi.org/10.1115/1.3211022
19. Yang, X.S., Deb, S.: Cuckoo search via Levy flights. In: World Congress on Nature and Biologically Inspired Computing (NaBIC), pp. 210–214. IEEE Publications, (2009)
20. Yang, X.S.: Nature-Inspired Metaheuristic Algorithms. Luniver Press, Frome (2008)
21. Yang, X.S., Deb, S., Fong, S.: Metaheuristic algorithms: optimal balance of intensification and diversification. Appl. Math. Inf. Sci. **8**(3), 977–983 (2014)
22. Fiser, I., Fister Jr., I., Yang, X.S., Brest, J.: A comprehensive review of firefly algorithms. Swarm. Evol. Comput. **13**(1), 34–46 (2013)
23. Yang, X.S., Xingshi, H.: Nature-Inspired Optimization Algorithms in Engineering Overview and Applications. Nature Inspired Computation in Engineering, pp. 1–20. Springer, Berlin (2016)
24. Bulatović, R.R., Đorđević, S.R., Đorđević, V.S.: Cuckoo search algorithm: a metaheuristic approach to solving the problem of optimum synthesis of a six-bar double dwell linkage. Mech. Mach. Theory **61**, 1–13 (2013)
25. Mezura-Montes, E., Portilla-Flores, E.A., Hernández-Ocaña, B.: Optimum synthesis of a four-bar mechanism using the modified bacterial foraging algorithm. Int. J. Syst. Sci. **45**(5), 1080–1100 (2014)
26. Bulatović, R.R., Miodragović, G., Bošković, M.S.: Modified krill herd (mkh) algorithm and its application in dimensional synthesis of a four-bar linkage. Mech. Mach. Theory **95**, 1–21 (2016)
27. Lin, W.Y., Hsiao, K.M.: Cuckoo search and teaching-learning-based optimization algorithms for optimum synthesis of path-generating four-bar mechanisms. J. Chin. Inst. Eng. **40**(1), 66–74 (2017)
28. Selvi, Ö., Yavuz, S.: Design and dimensional optimization of a novel walking mechanism with firefly algorithm. In: International Workshop on Computational Kinematics, pp. 67–75. Springer, Cham (2017)
29. Li, X., Wang, G., Miao, S., Li, X.: Optimal design of a hydraulic excavator working device based on parallel particle swarm optimization. J. Braz. Soc. Mech. Sci. (2017). https://doi.org/10.1007/s40430-017-0798-5
30. Sardashti, A., Daniali, H.M., Varedi, S.M.: Optimal free-defect synthesis of four-bar linkage with joint clearance using PSO algorithm. Meccanica **48**(7), 1681–1693 (2013)
31. Ebrahimi, S., Payvandy, P.: Efficient constrained synthesis of path generating four-bar mechanisms based on the heuristic optimization algorithms. Mech. Mach. Theory. **85**, 189–204 (2015)
32. Lee, C.T., Lee, C.C.: On a hybrid particle swarm optimization method and its application in mechanism design. Proc. Ins. Mech. Eng. C-J. Mech. **228**(15), 2844–2857 (2014)
33. Singh, R., Chaudhary, H., Singh, A.K.: Defect-free optimal synthesis of crank-rocker linkage using nature-inspired optimization algorithms. Mech. Mach. Theory **116**, 105–122 (2017)
34. Barthelemy, P., Bertolotti, J., Wiersma, D.S.: A Lévy-flight for light. Nature **453**, 495–498 (2008)
35. Brown, C., Liebovitch, L.S., Glendon, R.: Lévy-flights in Dobe Ju/'hoansi foraging patterns. Hum. Ecol. **35**, 129–138 (2007)
36. Lin, S.K.: Dynamics of the manipulator with closed chains. IEEE Trans. Robot. Autom. **6**, 496–501 (1990)
37. Lurie, A.I.: Notes on analytical mechanics. Prikladnaya Matematika i Mekhanika (PMM) **21**(6), 759–768 (1957). (in Russian)
38. Lurie, A.I.: Analytical Mechanics. Springer, Berlin (2002)
39. Wang, J.T., Huston, R.L.: Kane's equations with undetermined multipliers—application to constrained multibody systems. ASME J. Appl. Mech. **54**, 424–429 (1987)
40. Blajer, W.: On the determination of joint reactions in multibody mechanisms. ASME J. Mech. Des. **126**, 341–350 (2004)
41. Yang, S., Deb, S.: Cuckoo search: recent advances and applications. Neural Comput. Appl. **24**(1), 169–174 (2014)
42. Fister Jr., I., Fister, D., Fister, I.: A comprehensive review of cuckoo search: variants and hybrids. Int. J. Math. Model. Numer. Opitm. **4**(4), 387–409 (2013)
43. Shehab, M., Khader, A.T., Al-Betar, M.A.: A survey on applications and variants of the cuckoo search algorithm. Appl. Soft. Comput. (In Press) (2017). https://doi.org/10.1016/j.asoc.2017.02.034
44. Fister, I., Yang, X.S., Brest, J.: A comprehensive review of firefly algorithms. Swarm. Evol. Comput. **13**, 34–46 (2013)
45. Yang, X.S., Xingshi, H.: Firefly algorithm: recent advances and applications. Int. J. Swarm Intell. **1**(1), 36–50 (2013)